The 480 nm system of KRb: 1 $^3\Delta_1$, 4 $^1\Sigma^+$, and 5 $^1\Sigma^+$ States

Yonghoon Lee,[†] Youngjee Yoon,[||,⊥] Adnan Muhammad,[‡] Jin-Tae Kim,[‡] Sungyul Lee,[§] and Bongsoo Kim*[,||]

Department of Chemistry, Mokpo National University, Jeonnam 534-729, Korea, Department of Photonic Engineering, Chosun University, Gwangju 501-759, Korea, College of Environmental Science and Applied Chemistry, Kyunghee University, Gyeonggi-do 449-701, Korea, and Department of Chemistry, KAIST, Daejeon 305-701, Korea

Received: March 31, 2010; Revised Manuscript Received: June 1, 2010

We have investigated the KRb 480 nm system by mass-resolved resonance enhanced two-photon ionization in a cold molecular beam. The 1 $^3\Delta_1$, 4 $^1\Sigma^+$, and 5 $^1\Sigma^+ \leftarrow$ X $^1\Sigma^+$ transitions have been identified. For the 1 $^3\Delta_1$ and 5 $^1\Sigma^+$ states, the electronic term values and vibrational constants are determined experimentally for the first time. Potential energy curves of the 4 $^1\Sigma^+$ and 5 $^1\Sigma^+$ states undergo multiple avoided crossings with nearby $^1\Sigma^+$ states in the observed spectral region. For the 4 $^1\Sigma^+$ state, a vibrational numbering of the experimentally observed levels is suggested. Anomalies in vibronic structures of the 4 $^1\Sigma^+$ and 5 $^1\Sigma^+$ states are understood by comparison with high-level ab initio calculations currently available. The avoided crossing energies are also experimentally estimated.

1. Introduction

Heteronuclear alkali metal dimers have attracted strong interest from the chemistry and physics research communities investigating ultracold molecules.[1,2] They are ideal samples for fundamental research of dipolar interactions and ultracold chemistry, and are relevant to the realization of new possible quantum bits. Since the proposal of quantum computation with trapped polar molecules by DeMille,[3] there have been intensive efforts to produce dense clouds of ultracold heteronuclear alkali metal dimers. Recently, Ni et al.[4] and Ospelkaus et al.[5] reported efficient production of ultracold dense KRb through stimulated Raman adiabatic passage (STIRAP) following the formation of weakly bound Feshbach KRb. For efficient STIRAP, it is necessary to select a suitable intermediate level in an excited electronic state that possesses large transition dipole moments and favorable Franck−Condon (FC) factors with both the initial and final rovibrational levels in the a $^3\Sigma^+$ and X $^1\Sigma^+$ states, respectively.[4] In this regard, extension of current knowledge on the energy-level structures of electronically excited heteronuclear alkali metal dimers would be helpful for seeking more efficient routes to forming and detecting ultracold molecules.

KRb is one of the most frequently employed heteronuclear alkali metal dimers for the production of ultracold polar molecules. However, there is presently insufficient spectroscopic information on its excited electronic states. Since the early works of Walter and Barratt[6] and Beuc et al.[7] on the structureless band centered at 496 nm and on the diffuse bands at 597, 587, and 569 nm, respectively, seven excited electronic states of KRb (1 $^1\Pi$, 2 $^1\Pi$, 3 $^1\Pi$, 3 $^1\Sigma^+$, 2 $^3\Sigma^+$, 3 $^3\Sigma^+$, and 1 $^1\Delta$) have been experimentally identified by high-resolution spectroscopy in a heat-pipe oven[8−12] and mass-resolved resonance enhanced two-photon ionization (RE2PI) in a pulsed molecular beam.[13,14] The weak perturbation between the 1 $^1\Pi$ and 2 $^1\Pi$ states has been investigated experimentally[9] and theoretically.[15] Also, a strongly perturbed vibronic structure of the 3 $^1\Pi$ state was noted by Amiot et al.[12] For the singlet ground X $^1\Sigma^+$ state of KRb, the first high-resolution study was reported by Ross et al.,[16] and more recently, Amiot and Vergès determined the potential energy curve (PEC) up to the internuclear distance $R = 10$ Å.[17] Pashov et al. reported very accurate PECs of the X $^1\Sigma^+$ and a $^3\Sigma^+$ states close to the K(4s) + Rb(5s) asymptote by a coupled channels fitting of a large data set.[18] Meanwhile, long-range data on the 2 $^3\Pi$, 3 $^3\Sigma^+$, 4 $^3\Sigma^+$, 4 $^1\Sigma^+$, and 3 $^3\Pi$ states obtained via photoassociation (PA) spectroscopy were reported.[19,20]

Extensive high-level ab initio calculations on the electronic structures of KRb have been reported by Yiannopoulou et al.,[21] Park et al.,[22] and Rousseau et al.[23] Among these theoretical works, the most accurate one[23] agrees very well with experimental results. Both the predicted electronic term values, T_e, and the equilibrium internuclear distances, R_e, show discrepancies of less than 1% from the corresponding experimental values.[23] The theoretical and experimental values of ω_e agree within a few percent.[23] Furthermore, current ab initio calculations on the PECs of alkali metal dimers often predict the peculiar shape of a PEC due to avoided crossing (AC) with considerably dependable accuracy.[24,25]

In this work, we have investigated complicated vibronic structures of KRb near 480 nm by mass-resolved RE2PI spectroscopy in a cold molecular beam. The combination of RE2PI in a cold molecular beam and mass spectrometric detection has shown excellent performance, particularly in assigning complex spectra of alkali metal dimers contributed by multiple excited electronic states.[24,26−29] Using this experimental technique, the excitation spectra have been greatly simplified by cooling in a molecular beam and isotopomer-selective detection. Also, in most cases, the vibrational quantum numbers of the excited levels, v', can be easily assigned based on the isotope shifts of the vibronic term values, $T_{v'}$. Ab initio calculations of the electronic structures of alkali metal dimers

* To whom correspondence should be addressed. Fax: +82-42-350-2810. E-mail: bongsoo@kaist.ac.kr.
[†] Mokpo National University.
[‡] Chosun University.
[§] Kyunghee University.
[||] KAIST.
[⊥] Current address: Memory Division, Samsung Electronics Co., Ltd., Hwasung, Gyeonggi-do 445-701, Korea.

10.1021/jp1028799
Published on Web 06/30/2010

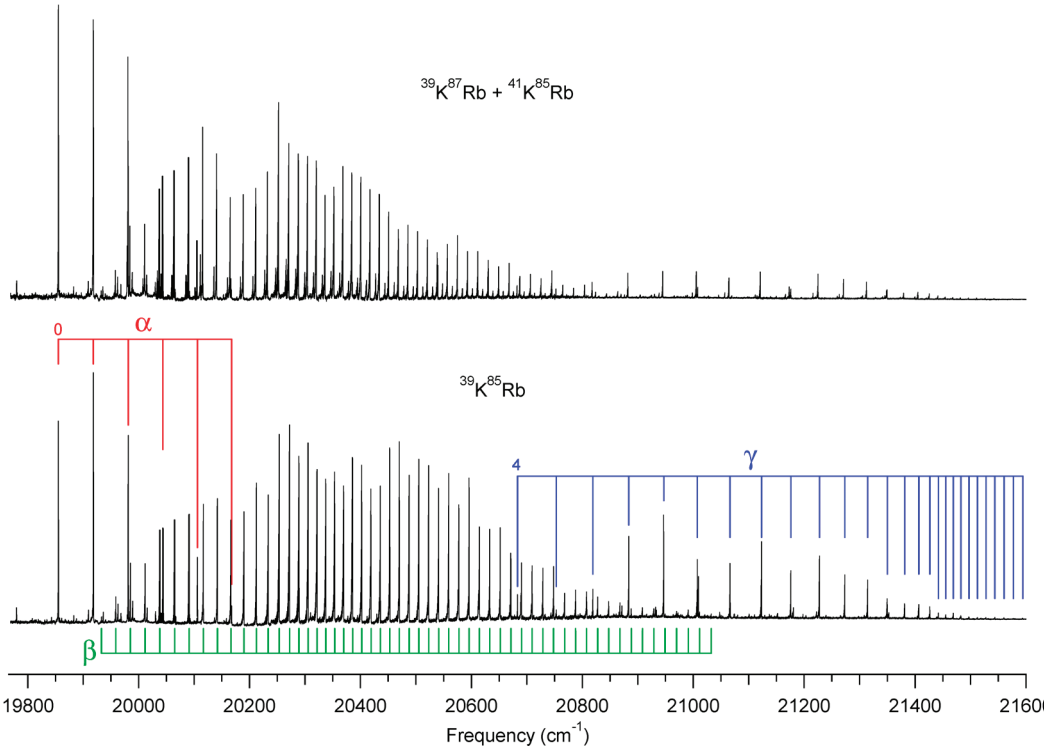

Figure 1. Low-resolution RE2PI spectra recorded at the channels of m/z = 124 ($^{39}K^{85}Rb$) and 126 ($^{39}K^{87}Rb$ and $^{41}K^{85}Rb$) between 19 750 and 21 600 cm^{-1} obtained by coexpanding Kr carrier gas. The three vibrational progressions are denoted as α, β, and γ. The v' numbers of the lowest-lying α and γ bands are noted. The majority of the minor features not shown as assigned in these spectra are in fact assignable to $v'' = 1$ hot bands (see Supporting Information).

predict that the density of states becomes larger as the excitation energy increases. Thus, simplification of the excitation spectra becomes more important in investigation of high-lying electronically excited states.

Herein, we report the observation and identification of the KRb 1 $^3\Delta_1$, 4 $^1\Sigma^+$, and 5 $^1\Sigma^+ \leftarrow$ X $^1\Sigma^+$ transitions. The three excited electronic states show characteristic vibronic structures. For the 1 $^3\Delta_1$ and 5 $^1\Sigma^+$ states, the T_e values and vibrational constants (ω_e, $\omega_e x_e$, and $\omega_e y_e$) have been determined experimentally for the first time. Multiple ACs of the 4 $^1\Sigma^+$ and 5 $^1\Sigma^+$ PECs have also been identified. The resulting abnormal vibronic structures have been elucidated by comparison with those calculated using the ab initio PECs from ref 23. The AC energies of the 4 $^1\Sigma^+$ and 5 $^1\Sigma^+$ PECs have been estimated experimentally. Furthermore, the observed levels in this work can be selected as an intermediate level for detecting photoassociated KRb[30] and ultracold KRb in the X $^1\Sigma^+$ $v = 0$ level by one-color RE2PI.

2. Experiment

Details of our experimental apparatus and techniques have been discussed previously.[31] Briefly, KRb was produced by expanding K and Rb vapor with Kr gas through a high-temperature pulsed nozzle with an 800 μm diameter orifice. The alkali metal sample was heated to 300 °C. The pulsed jet was collimated by a 1.2 mm diameter skimmer. From the naturally occurring isotopes of K (^{39}K and ^{41}K) and Rb (^{85}Rb and ^{87}Rb), four different isotopomers of KRb ($^{39}K^{85}Rb$, 67.3%; $^{39}K^{87}Rb$, 26.0%; $^{41}K^{85}Rb$, 4.9%; $^{41}K^{87}Rb$, 1.9%) were produced in the molecular beam. Two photons from a Nd:YAG pumped dye laser excited and ionized KRb. The resulting ions of isotopomers were separately and simultaneously detected by a linear time-of-flight (TOF) mass spectrometer ($m/\Delta m \approx 500$). The ion signals at the channels of the mass-to-charge ratio, m/z = 124 ($^{39}K^{85}Rb^+$) and 126 ($^{39}K^{87}Rb^+$ and $^{41}K^{85}Rb^+$), were recorded. Although the mass spectra of $^{39}K^{87}Rb^+$ and $^{41}K^{85}Rb^+$ could not be separated, their vibronic bands were clearly resolved by isotope shifts. The vibronic structures were revealed by a laser resolution of 0.12 cm^{-1} ($\Delta\nu_{fwhm}$). Wavelength calibration of the dye laser was conducted using Ne and Ar optogalvanic spectra.

3. Results and Discussion

Figure 1 shows low-resolution RE2PI spectra recorded at the channels of m/z = 124 ($^{39}K^{85}Rb^+$) and 126 ($^{39}K^{87}Rb^+$ and $^{41}K^{85}Rb^+$), between 19 750 and 21 600 cm^{-1} obtained by Kr carrier gas. The observed vibronic structures consist of three main vibrational progressions, denoted as α, β, and γ in Figure 1. Band positions of $^{39}K^{85}Rb$, $^{39}K^{87}Rb$, and $^{41}K^{85}Rb$ are listed in the Supporting Information. The initial level of the observed vibronic transitions is identified by the energy difference between the $v' \leftarrow v'' = 0$ and $v' \leftarrow v'' = 1$ bands with a common upper vibronic level. The energy difference between the v'' = 1 and 0 levels of the X $^1\Sigma^+$ state, $G_{v''=1} - G_{v''=0}$ = 75.3848 cm^{-1}, is calculated from the Dunham coefficients reported by Amiot and Vergès using high-resolution Fourier transform spectroscopy (FTS).[17] The assignment of hot bands of α and β progressions is listed in the Supporting Information. The observed energy difference between the original and hot bands is 75.429(58) cm^{-1}, agreeing well with the X $^1\Sigma^+$ $G_{v''=1} - G_{v''=0}$ values from high-resolution FTS.[17] Therefore, the initial vibronic level of the observed progressions is identified as the X $^1\Sigma^+$ v'' = 0 level.

Figure 2 shows the nonrelativistic ab initio PECs of the 1 $^3\Delta$, 4 $^1\Sigma^+$, 5 $^1\Sigma^+$, 6 $^1\Sigma^+$, 4 $^3\Sigma^+$, 5 $^3\Sigma^+$, and 3 $^3\Pi$ states.[23] The vertical dotted line represents the FC region excited from the X $^1\Sigma^+$ $v'' = 0$ level. Between 20 000 and 22 000 cm^{-1}, the

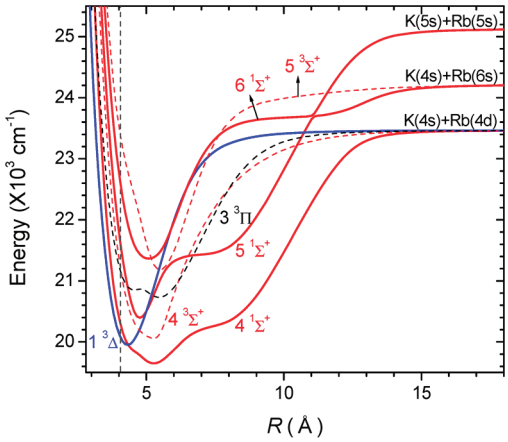

Figure 2. Nonrelativistic ab initio PECs of KRb for the 1 $^3\Delta$, 4 $^1\Sigma^+$, 5 $^1\Sigma^+$, 6 $^1\Sigma^+$, 4 $^3\Sigma^+$, 5 $^3\Sigma^+$, and 3 $^3\Pi$ states. The vertical dotted line represents the FC region (R_e of the X $^1\Sigma^+$ state, 4.055 Å from ref 23). The origin of the ordinate axis is set to the potential minimum of the X $^1\Sigma^+$ state.

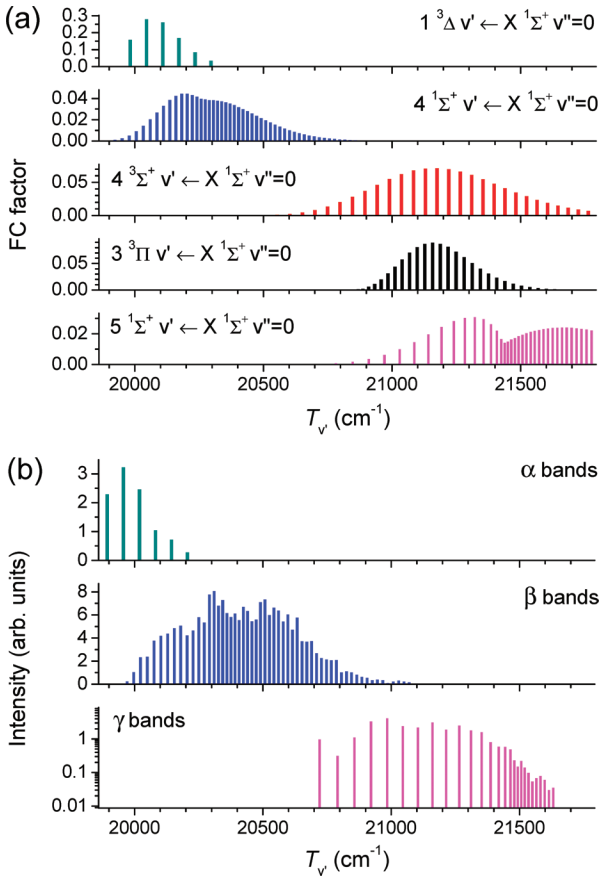

Figure 3. (a) FC factors of the 1 $^3\Delta$, 4 $^1\Sigma^+$, 4 $^3\Sigma^+$, 3 $^3\Pi$, and 5 $^1\Sigma^+ \leftarrow$ X $^1\Sigma^+$ $v = 0$ transitions, calculated using the ab initio PECs from ref 23. (b) Observed vibronic-band intensity distributions of α, β, and γ progressions.

inner walls of the 1 $^3\Delta$, 4 $^1\Sigma^+$, 3 $^3\Pi$, 4 $^3\Sigma^+$, and 5 $^1\Sigma^+$ PECs are predicted to be in the FC region. Figure 3 shows plots of (a) the FC factors of the transitions to the 1 $^3\Delta$, 4 $^1\Sigma^+$, 4 $^3\Sigma^+$, 3 $^3\Pi$, and 5 $^1\Sigma^+$ vibronic levels from the X $^1\Sigma^+$ $v'' = 0$ level, and (b) experimentally observed intensities of the α, β, and γ bands as functions of $T_{v'}$ (=T_e + $G_{v'}$). The FC factors and $T_{v'}$ values shown in Figure 3a were calculated by the LEVEL 7.7 program[32] using the ab initio PECs.[23] From a comparison of the FC-region energy and the vibrational spacing between the

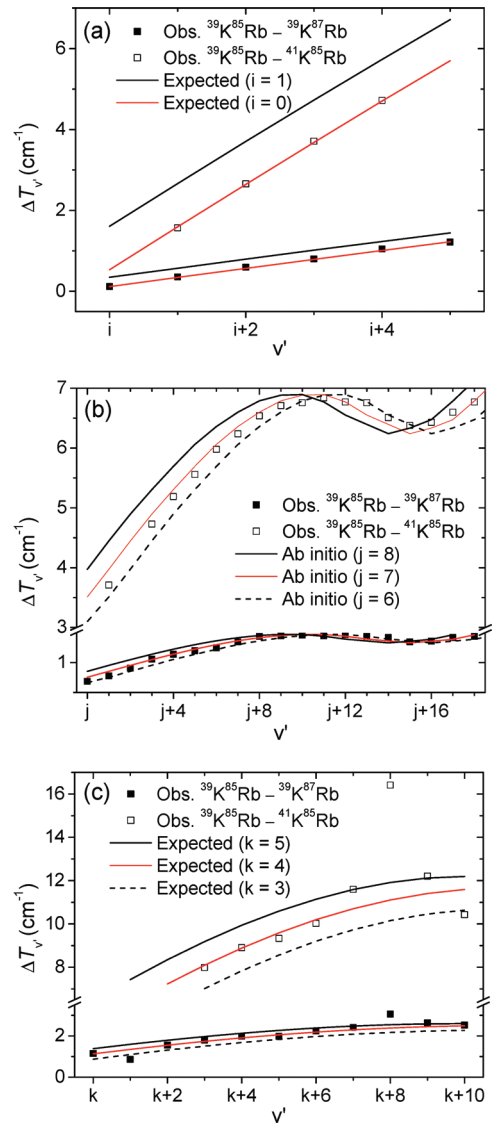

Figure 4. Comparisons of observed and expected isotope shifts of (a) α, (b) β, and (c) γ bands. For the α and γ bands, the expected isotope shifts were calculated from the fitted molecular constants with the v' assignments as noted in panels a and c. For the β bands, the expected isotope shifts were calculated using the ab initio PEC of the 4 $^1\Sigma^+$ state from ref 23.

theoretically predicted structures and the experimentally observed ones, we assigned the upper electronic states of the α, β, and γ bands to the 1 $^3\Delta$, 4 $^1\Sigma^+$, and 5 $^1\Sigma^+$ states, respectively. In Figure 2, the PECs of the 1 $^3\Delta$ state have the closest R_e to that of the X $^1\Sigma^+$ state among the excited electronic states. According to the ab initio calculation, R_e of the 1 $^3\Delta$ state is 4.316 Å and that of the X $^1\Sigma^+$ state is 4.055 Å. If $R_e' \approx R_e''$, the $v' = 0 \leftarrow v'' = 0$ transition shows the strongest intensity (FC factor) and the intensities of the $v' = 1, 2, 3, \ldots \leftarrow v'' = 0$ transitions decrease rapidly. For the FC factors of the 1 $^3\Delta$ $v' \leftarrow$ X $^1\Sigma^+$ $v'' = 0$ transition shown in Figure 3a, v' of the lowest-lying band ($T_{v'}$ = 19 981.8 cm^{-1}) is 0. By comparing the FC factors of 1 $^3\Delta$−X $^1\Sigma^+$ in Figure 3a and the observed intensities of α bands in Figure 3b, we find that the variation of FC factors with v' agrees well with the distribution of the α band intensities. Considering the accuracy of the theoretical calculation,[23] this agreement seems to provide dependable assignment of the v' values of the α bands as well as the upper electronic state.

Figure 4 shows the observed isotope shifts, $\Delta T_{v'}$ (=$T_{v'}$(^{39}K^{85}Rb) − $T_{v'}$(^{39}K^{87}Rb) and $T_{v'}$(^{39}K^{85}Rb) − $T_{v'}$(^{41}K^{85}Rb)),

TABLE 1: Experimental and Theoretical Molecular Constants of the KRb 1 $^3\Delta$, 4 $^1\Sigma^+$, 5 $^1\Sigma^+$, 4 $^3\Sigma^+$, and 3 $^3\Pi$ States

		T_e (cm^{-1})	ω_e (cm^{-1})	$\omega_e x_e$ (cm^{-1})	$\omega_e y_e$ (cm^{-1})	R_e (Å)
α [1 $^3\Delta_1$]		19 861.535(24)	63.296(34)	0.081(13)	−0.0099(14)	
γ [5 $^1\Sigma^+$]		20 394.6(37)	75.6(14)	0.56(16)	−0.0195(57)	
1 $^3\Delta$	theory 1[a]	19 950	64.0			4.316
	theory 2[b]	20 124	64			4.37
4 $^1\Sigma^+$	theory 1[a]	19 648	38.6			5.265
	theory 2[b]	19 611	38			5.30
5 $^1\Sigma^+$	theory 1[a]	20 393	75.7			4.761
	theory 2[b]	20 339	75			4.80
4 $^3\Sigma^+$	theory 1[a]	20 060	43.7			5.275
	theory 2[b]	19 981	59			5.30
3 $^3\Pi$	theory 1[a]	20 729	40.5			5.413
	theory 2[b]	20 732	38			5.45

[a] Reference 23. [b] Reference 22.

of the (a) α, (b) β, and (c) γ bands. For the β and γ bands, the $\Delta T_{v'}$ values of the lowest 20 and 11 levels, respectively, are plotted. The observed $\Delta T_{v'}$ values of the α and γ bands are compared with the calculated values from the fitted molecular constants. The observed values of the β bands are compared with the calculated values from the ab initio 4 $^1\Sigma^+$ PEC.[23,32] For the α and γ bands, the v' values are clearly assigned. The observed vibronic term values, $T_{v'}$ (=band origin + $G_{v''=0}$), of the isotopomers are fitted simultaneously by the following equation.

$$T_{v'} = T_e + \omega_e\rho(v' + 1/2) - \omega_e x_e[\rho(v' + 1/2)]^2 + \omega_e y_e[\rho(v' + 1/2)]^3 + ...$$

The value of the constant ρ is 1 for ^{39}K^{85}Rb, 0.996 378 990 for ^{39}K^{87}Rb, and 0.983 139 464 for ^{41}K^{85}Rb,[33] and is given by $(\mu/\mu_{iso})^{1/2}$, where μ and μ_{iso} are the reduced masses of the major isotopomer (^{39}K^{85}Rb) and the minor isotopomers (^{39}K^{87}Rb and ^{41}K^{85}Rb), respectively. The $\Delta T_{v'}$ values are then calculated using the fitted T_e and vibrational constants, ω_e, $\omega_e x_e$, and $\omega_e y_e$, using the following equation.

$$\Delta T_{v'} = \omega_e(v' + 1/2) - \omega_e x_e\rho(v' + 1/2)^2 + \omega_e y_e\rho(v' + 1/2)^3 + ... - \{\omega_e\rho(v' + 1/2) - \omega_e x_e[\rho(v' + 1/2)]^2 + \omega_e y_e[\rho(v' + 1/2)]^3 + ...\}$$

The v' values of the lowest-lying α and γ bands, i and k, are assigned to 0 and 4, respectively. The $\Delta T_{v'}$ values estimated by these assignments show the best agreement with the observed values (see Figure 4a,c). The v' values of the higher-lying bands were assigned successively. For fitting α bands, the $v' = 0-5 \leftarrow v'' = 0$ bands of ^{39}K^{85}Rb and ^{39}K^{87}Rb and the $v' = 1-4 \leftarrow v'' = 0$ bands of ^{41}K^{85}Rb were included in the data set. For fitting γ bands, the $v' = 4-13 \leftarrow v'' = 0$ bands of ^{39}K^{85}Rb and ^{39}K^{87}Rb were included. The band-origin positions obtained by rotational band contour fits were converted to the $T_{v'}$ values. The experimentally determined molecular constants and theoretical values are listed in Table 1. By comparing the experimental and theoretical values of T_e and ω_e, the upper electronic states of α and γ bands were consistently assigned to the 1 $^3\Delta$ and 5 $^1\Sigma^+$ states, respectively.

However, the v' values and molecular constants of the β bands could not be assigned from the observed isotope shifts due to the peculiar shape of the 4 $^1\Sigma^+$ PEC in the observed spectral region. Ab initio calculations show clear ACs of the inner and outer walls of the 4 $^1\Sigma^+$ PEC around 19 950 and 20 240 cm^{-1}, respectively (Figure 2). The lower-lying AC was not observed in our experiment due to negligible FC factors in that energy region. The observed β progression corresponds to transitions to the 4 $^1\Sigma^+$ PEC above the lower-lying AC energy. Therefore, the molecular constants determined from the observed β bands cannot describe the energy-level structure in the 4 $^1\Sigma^+$ PEC below ~19 950 cm^{-1}. Although T_e and vibrational constants of the 4 $^1\Sigma^+$ state could not be determined, comparison of the observed isotope shifts of the β bands with the calculated values from the ab initio 4 $^1\Sigma^+$ PEC provides convincing assignment of v' values (see Figure 4b). For the lowest-lying β band at 19 933.0 cm^{-1}, the most probable v' is estimated to be 7 ($j = 7$; j is v' of the lowest-lying β band) with an uncertainty of $\Delta v' = \pm 1$, and the v' values of the higher-lying β bands are assigned successively. The uncertainty of this vibrational numbering depends on the accuracy of the ab initio 4 $^1\Sigma^+$ PEC. Taking the accuracy of the ab initio calculation[23] into consideration, the uncertainty of v' would be a few quanta. Previously, Wang et al. observed the vibrational levels of the 4 $^1\Sigma^+$ state through the transition from the highly excited vibrational levels in the X $^1\Sigma^+$ state ($v'' = 89$ and others) using PA spectroscopy.[19] The $T_{v'}$ and $\Delta G_{v'}$ values obtained in our work and those reported in ref 19 are compared in the Supporting Information. Our results agree well with those of Wang et al. They also proposed very convincing vibrational numbering of the observed 4 $^1\Sigma^+$ levels by comparing the observed term values and vibrational spacing with those calculated using the ab initio 4 $^1\Sigma^+$ PEC. The v' of the lowest lying level, v'_{MIN}, observed in their experiment was assigned as $25 \leq v'_{MIN} \leq 33$. The v' of the corresponding level observed in our experiment is assigned as 31 with a minimum uncertainty of $\Delta v' = \pm 1$ by comparing the observed and calculated isotope shifts. Wang et al. and we use the same ab initio 4 $^1\Sigma^+$ PEC from ref 23 for the calculations.

Although the FC factors of the 4 $^3\Sigma^+$ and 3 $^3\Pi \leftarrow$ X $^1\Sigma^+$ $v'' = 0$ transitions are predicted to be comparable to or larger than those of the observed 4 $^1\Sigma^+$ and 5 $^1\Sigma^+ \leftarrow$ X $^1\Sigma^+$ $v'' = 0$ transitions (see Figure 3a), transitions to the 4 $^3\Sigma^+$ and 3 $^3\Pi$ states were not observed in our experiment. This indicates that these triplet states are not significantly mixed with singlet states, and thus the triplet−singlet transitions are strictly forbidden. Wang et al. observed transitions to the 4 $^3\Sigma^+$ and 3 $^3\Pi$ states from the a $^3\Sigma^+$ state.[19]

The upper electronic states of the α, β, and γ bands were assigned to the 1 $^3\Delta$, 4 $^1\Sigma^+$, and 5 $^1\Sigma^+$ states, respectively, by analyzing their vibronic structures. For the 1 $^3\Delta$ state, the electronic state is split into three, $\Omega = 1$, 2, and 3, component

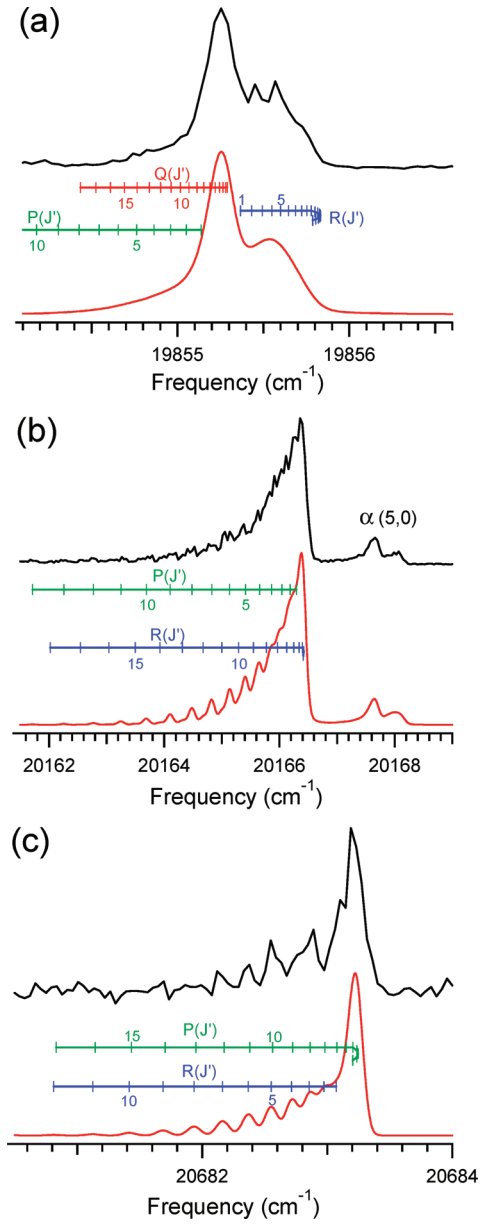

Figure 5. Experimentally observed and simulated rotational contour spectra of (a) α ($v' = 0 \leftarrow v'' = 0$), (b) β ($v' = j + 9 \leftarrow v'' = 0$), and (c) γ ($v' = 4 \leftarrow v'' = 0$) bands of $^{39}K^{85}Rb$. The experimental spectra were recorded by coexpanding with Kr carrier gas at 600, 400, and 460 Torr for the α, β, and γ bands. The optimized band parameters are listed in Table 2.

states due to spin−orbit interaction (Λ(2) + Σ(−1, 0, and 1), where Λ and Σ are the projections of the total electronic orbital angular momentum and the total electron spin onto the internuclear axis, respectively). Among these three Ω states, only the Ω = 1 state can be excited from the X $^1\Sigma^+$ state (Ω = 0), through a perpendicular transition dipole moment (ΔΩ = ± 1). Transitions to other components are forbidden by the selection rule. On the other hand, the 4 $^1\Sigma^+$ and 5 $^1\Sigma^+$ states are excited from the X $^1\Sigma^+$ state through a parallel transition dipole moment (ΔΩ = 0). From the rotational contours of the spectra, the Ω symmetries of the upper electronic states can be determined. Parallel bands consist of rotational P (ΔJ = −1) and R (ΔJ = 1) branches of comparable intensity, while perpendicular bands show a strong Q (ΔJ = 0) branch with approximately 2-fold greater intensity than that of the P and R branches.[33] Figure 5 shows the rotational contour spectra of the

TABLE 2: Band Parameters of α ($v' = 0 \leftarrow v'' = 0$), β ($v' = j + 9 \leftarrow v'' = 0$), and γ ($v' = 4 \leftarrow v'' = 0$) Bands Optimized by Rotational Contour Fits

	α (0, 0)	β (j + 9, 0)	γ (4, 0)
band origin (cm^{-1})	19 855.2949(15)	20 166.3705(17)	20 683.1516(46)
$B_{v'}$ (cm^{-1})	0.035 558(60)	0.021 348(70)	0.027 27(22)
T_{rot} (K)	1.263(19)	2.010(32)	1.76(12)
$\Delta\nu_{Gauss}$[a] (cm^{-1})	0.12	0.12	0.12
$\Delta\nu_{Lorent}$[b] (cm^{-1})	0.0450(28)	0.0542(42)	
$\langle R\rangle_{v'}$[c] (Å)	4.226	5.455	4.826
R_e[d] (Å)	4.316 (1 $^3\Delta$)	5.265 (4 $^1\Sigma^+$)	4.761 (5 $^1\Sigma^+$)

[a] Fixed. [b] Not included in the contour fit of the γ (4, 0) band. [c] Equilibrium bond length at the vibrational level calculated from $\langle R\rangle_{v'} = [(\hbar^2/2)(1/hc)(1/\mu B_{v'})]^{1/2}$. [d] Reference 23.

(a) α ($v' = 0 \leftarrow v'' = 0$), (b) β ($v' = j + 9 \leftarrow v'' = 0$), and (c) γ ($v' = 4 \leftarrow v'' = 0$) bands and their simulations. The experimental spectra of the α, β, and γ bands were recorded by coexpanding with Kr carrier gas at 600, 400, and 460 Torr, respectively. The experimental spectra were analyzed by contour fits and simulated using the PGOPHER program.[34] The optimized band parameters are listed in Table 2. Figure 5a shows that the α band is simulated well assuming the perpendicular transition (P, Q, and R branches). The strong central peak is due to accumulation of Q-branch rotational lines with low J' values. This indicates that the upper electronic state of the α band is the 1 $^3\Delta_1$ state. For the β and γ bands, the $^1\Sigma^+ - ^1\Sigma^+$ parallel transitions were confirmed by the rotational structures (P and R branches) (see Figure 5b,c). Note that the rotational constants ($B_{v'}$) used to model the bands of the α, β, and γ systems are consistent with the R_e values of the ab initio 1 $^3\Delta$, 4 $^1\Sigma^+$, and 5 $^1\Sigma^+$ PECs (compare the experimental $\langle R\rangle_{v'}$ and theoretical R_e values in Table 2).

We have thus far identified the vibronic structures of the α, β, and γ bands. In the following, the effects of ACs of the 4 $^1\Sigma^+$ and 5 $^1\Sigma^+$ PECs on their vibronic structures are discussed. Among the observed excited electronic states, the 4 $^1\Sigma^+$ and 5 $^1\Sigma^+$ states show PECs having peculiar shapes (Figure 2). This is due to the cascade ACs caused by several $^1\Sigma^+$ states. The shape of a PEC changes abruptly around the AC energy, and there appear to be discontinuities in the R-dependent properties such as the rotational constant and vibrational frequency. Figure 6 shows the observed and calculated vibrational spacing, $\Delta G_{v'}$ (=$G_{v'+1} - G_{v'}$), and $\Delta T_{v'}$ of the 4 $^1\Sigma^+$ and 5 $^1\Sigma^+$ states as a function of $T_{v'}$. The calculated values were obtained by the LEVEL 7.7 program[28] and the ab initio PECs of the 4 $^1\Sigma^+$ and 5 $^1\Sigma^+$ states.[20] As shown in Figure 6, the observed irregularities in $\Delta G_{v'}$ and $\Delta T_{v'}$ of the 4 $^1\Sigma^+$ and 5 $^1\Sigma^+$ states are superbly reproduced by the calculation using the ab initio PECs. The irregularities in the calculated $\Delta G_{v'}$ and $\Delta T_{v'}$ values are indicated by red arrows, and the experimentally observed irregularities are indicated by black arrows. The insets of parts and and c of Figure 6 show the ab initio PECs of the 4 $^1\Sigma^+$ and 5 $^1\Sigma^+$ states from ref 23, respectively. In the insets, the ACs of the PECs are also indicated by red arrows. For the 4 $^1\Sigma^+$ state, irregularities in the vibrational structure are predicted at 19 950 and 20 240 cm^{-1}. From the 4 $^1\Sigma^+$ PEC, the low-lying irregularity originates from the AC of the inner PEC rim and the high-lying irregularity from the AC of the outer PEC rim. "I" and "O" denote the ACs of the inner and outer PEC rims, respectively, in Figure 6a,c. From the experimental results it is estimated that the AC energy of the outer PEC rim is 20 310 cm^{-1} (indicated by the black arrow in Figure 6a). The lower-lying irregularity of $\Delta G_{v'}$ and $\Delta T_{v'}$ in the β progression was not fully observed. The AC energy corresponds to the lower

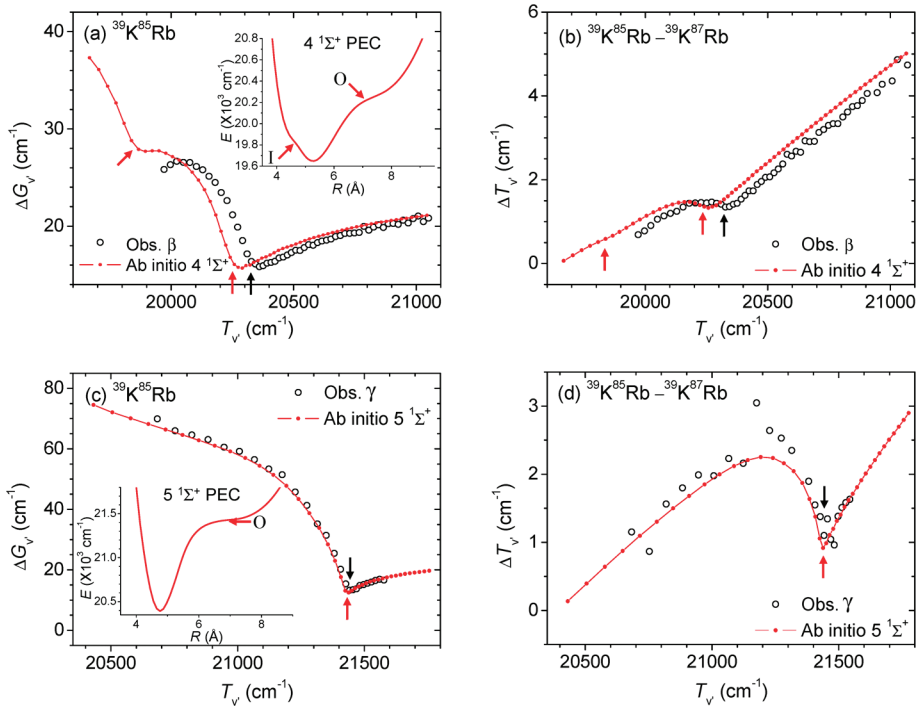

Figure 6. Comparisons of $\Delta G_{v'}$ and $\Delta T_{v'}$ values of β and γ bands and those calculated from ab initio PECs of the 4 $^1\Sigma^+$ and 5 $^1\Sigma^+$ states. The irregularities in $\Delta G_{v'}$ and $\Delta T_{v'}$ are indicated by arrows. The insets of (a) and (c) show the 4 $^1\Sigma^+$ and 5 $^1\Sigma^+$ PECs (from ref 23), respectively. The ACs of the PECs are also indicated by arrows.

edge of the FC envelope. However, it is estimated to be located at around 20 020 cm^{-1} based on the shift of the observed AC energy from the theoretical AC energy of the outer PEC rim (70 cm^{-1}). For the 5 $^1\Sigma^+$ state, the theoretically calculated and experimentally observed AC energies of the outer PEC rim match very well (see Figure 6c). The AC energy of the outer 5 $^1\Sigma^+$ PEC rim is 21 400 cm^{-1}.

4. Conclusion

We have identified the KRb 1 $^3\Delta_1$, 4 $^1\Sigma^+$, and 5 $^1\Sigma^+$ states by mass-resolved RE2PI in a cold molecular beam for the first time. For the 1 $^3\Delta_1$ and 5 $^1\Sigma^+$ states, T_e and vibrational constants were experimentally determined. From a rotational contour analysis, the Ω symmetries of the upper electronic states of the observed bands were assigned. The 4 $^1\Sigma^+$ and 5 $^1\Sigma^+$ states show PECs of peculiar shapes due to ACs by nearby $^1\Sigma^+$ states. These lead to irregularities in their vibronic structures. The ab initio 4 $^1\Sigma^+$ and 5 $^1\Sigma^+$ PECs successfully reproduced the irregularities of the observed vibronic structures. The AC energies of the 4 $^1\Sigma^+$ and 5 $^1\Sigma^+$ PECs were estimated from the observed vibronic structures. Our results can be complementary to those reported by Wang et al.[19] We investigated the vibronic structures of the KRb 480 nm system in the region around R_e of the X $^1\Sigma^+$ state through the transitions from the X $^1\Sigma^+$ $v'' = 0$ level. Wang et al. investigated the same energy region in a longer range of R through the transitions from the a $^3\Sigma^+$ $v'' = 20$ and 21 and X $^1\Sigma^+$ $v'' = 89$ and other levels. The combined results will be useful for seeking efficient routes for formation and detection of ultracold KRb molecules.

Acknowledgment. This work was supported by NRF Grants (2009-0071746, 2010-0001484, 2009-0085319, 20090083138, 20090063004) from the Korean Government. S.L. thanks the MEST, Korea (Converging Research Program, 2009-0081952), for financial support.

Supporting Information Available: Data of the KRb 480 nm system by RE2PI spectroscopy: (i) band positions of the α, β, and γ progressions of ^{39}K^{85}Rb, ^{39}K^{87}Rb, and ^{41}K^{85}Rb isotopomers; (ii) assignment of hot bands of α and β progressions; (iii) $T_{v'}$ values and (iv) $\Delta G_{v'}$ plots of our work and of Wang et al.[19] This material is available free of charge via the Internet at http://pubs.acs.org.

References and Notes

(1) Stwalley, W. C.; Banerjee, J.; Bellos, M.; Carollo, R.; Recore, M.; Mastroianni, M. *J. Phys. Chem. A* **2010**, *114*, 81.
(2) Carr, L. D.; DeMille, D.; Krems, R. V.; Ye, J. *New J. Phys.* **2009**, *11*, 055049.
(3) DeMille, D. *Phys. Rev. Lett.* **2002**, *88*, 067901.
(4) Ni, K.-K.; Ospelkaus, S.; de Miranda, M. H. G.; Pe'er, A.; Neyenhuis, B.; Zirbel, J. J.; Kotochigova, S.; Julienne, P. S.; Jin, D. S.; Ye, J. *Science* **2008**, *322*, 231.
(5) Ospelkaus, S.; Pe'er, A.; Ni, K.-K.; Zirbel, J. J.; Neyenhuis, B.; Kotochigova, S.; Julienne, P. S.; Ye, J.; Jin, D. S. *Nat. Phys.* **2008**, *4*, 622.
(6) Walter, J. M.; Baratt, S. *Proc. R. Soc. London, Ser. A* **1928**, *119*, 257.
(7) Beuc, R.; Milosevic, S.; Pichler, G. *J. Phys. B* **1984**, *17*, 739.
(8) Okada, N.; Kasahara, S.; Ebi, T.; Baba, M.; Kato, H. *J. Chem. Phys.* **1996**, *105*, 3458.
(9) Kasahara, S.; Fujiwara, C.; Okada, N.; Kato, H. *J. Chem. Phys.* **1999**, *111*, 8857.
(10) Amiot, C. *J. Mol. Spectrosc.* **2000**, *203*, 126.
(11) Amiot, C.; Vergès, J.; Effantin, C.; d'Incan, J. *Chem. Phys. Lett.* **2000**, *321*, 21.
(12) Amiot, C.; Vergès, J.; d'Incan, J.; Effantin, C. *Chem. Phys. Lett.* **1999**, *315*, 55.
(13) Lee, Y.; Yun, C.; Yoon, Y.; Kim, T.; Kim, B. *J. Chem. Phys.* **2001**, *115*, 7413.
(14) Lee, Y.; Yoon, Y.; Kim, B.; Li, L.; Lee, S. *J. Chem. Phys.* **2004**, *120*, 6551.
(15) Leininger, T.; Stoll, H.; Jeung, G.-H. *J. Chem. Phys.* **1997**, *106*, 2541.
(16) Ross, A. J.; Effanfin, C.; Crozet, P.; Boursey, E. *J. Phys. B* **1990**, *23*, L247.
(17) Amiot, C.; Vergès, J. *J. Chem. Phys.* **2000**, *112*, 7068.
(18) Pashov, A.; Docenko, O.; Tamanis, M.; Ferber, R.; Knöckel, H.; Tiemann, E. *Phys. Rev. A* **2007**, *76*, 022511.

(19) Wang, D.; Eyler, E. E.; Gould, P. L.; Stwalley, W. C. *J. Phys. B: At. Mol. Opt. Phys.* **2006**, *39*, S849.

(20) Kim, J. T.; Wang, D.; Eyler, E. E.; Gould, P. L.; Stwalley, W. C. *New J. Phys.* **2009**, *11*, 055020.

(21) Yiannopoulou, A.; Leininger, T.; Lyyra, A. M.; Jeung, G.-H. *Int. J. Quantum Chem.* **1996**, *57*, 575.

(22) Park, S. J.; Choi, Y. J.; Lee, Y. S.; Jeung, G.-H. *Chem. Phys.* **2000**, *257*, 135.

(23) Rousseau, S.; Allouche, A. R.; Aubert-Frécon, M. *J. Mol. Spectrosc.* **2000**, *203*, 235.

(24) Yoon, Y.; Lee, Y.; Kim, T.; Jeung, S. A.; Jung, Y.; Kim, B.; Lee, S. *J. Chem. Phys.* **2001**, *114*, 8926.

(25) Allouche, A. R.; Korek, M.; Fakherddin, K.; Chaalan, A.; Dagher, M.; Taher, F.; Aubert-Frécon, M. *J. Phys. B: At. Mol. Opt. Phys.* **2000**, *33*, 2307.

(26) Lee, Y.; Lee, S.; Kim, B. *J. Phys. Chem. A* **2007**, *111*, 11750.

(27) Lee, Y.; Lee, S.; Kim, B. *J. Phys. Chem. A* **2008**, *112*, 6893.

(28) Lee, Y.; Yoon, Y.; Lee, S.; Kim, J.-T.; Kim, B. *J. Phys. Chem. A* **2008**, *112*, 7214.

(29) Lee, Y.; Yoon, Y.; Lee, S.; Kim, B. *J. Phys. Chem. A* **2009**, *113*, 12187.

(30) Wang, D.; Eyler, E. E.; Gould, P. L.; Stwalley, W. C. *Phys. Rev. Lett.* **2005**, *72*, 032502.

(31) Lee, Y.; Yoon, Y.; Baek, S. J.; Joo, D.-L.; Ryu, J.; Kim, B. *J. Chem. Phys.* **2000**, *113*, 2116.

(32) Le Roy, R. J. *LEVEL 7.7. A Computer Program for Solving the Radial Schrödinger Equation for Bound and Quasibound Levels*; University of Waterloo Chemical Physics Research Report CP-661; University of Waterloo: Ontario, Canada, 2005.

(33) Lefebvre-Brion, H.; Field, R. W. *The Spectra and Dynamics of Diatomic Molecules*; Elsevier: New York, 2004.

(34) Western, C. M. *PGOPHER version 5.2, a Program for Simulating Rotational Structure*; University of Bristol: Bristol, U.K., 2007; http://pgopher.chm.bris.ac.uk.

JP1028799